Journal of Craniomaxillofacial Research

Vol. 13, Issue. 3 Summer 2026

Accuracy of Photogrammetry in Full-Arch Implant Rehabilitation: A Systematic Review

Afsane Mokhtari [1], Ali Mirzaei [1], Alireza Ghaffarian Hosseini [1], Amirtaher Mirmortazavi [2*]

1. Student Research Committee, Mashhad School of Dentistry, Mashhad University of Medical Sciences, Mashhad, Iran.

2. Oral and Maxillofacial Diseases Research Center, Mashhad University of Medical Sciences, Mashhad, Iran.

ARTICLE INFO

Article Type:
Systematic Review

Received: 9 February 2026
Revised: 8 April 2026
Accepted: 20 June 2026

**Corresponding author:*
Amirtaher Mirmortazavi

Oral and Maxillofacial Diseases Research Center, Mashhad University of Medical Sciences, Mashhad, Iran.

Tel: +98-21-84903747
Fax: +98-21-84903747
Email: mirmortazaviat@gmail.com

ABSTRACT

Introduction: Precise transfer of implant positions is critical for the success of full-arch rehabilitations. Photogrammetry-based workflows aim to mitigate the cumulative stitching errors common in intraoral scanning (IOS), though performance varies across different systems and protocols. To evaluate the accuracy (trueness and precision) of photogrammetry for edentulous complete-arch implant capture compared to IOS and conventional impressions.

Materials and Methods: PubMed, Web of Science, Scopus, and Embase were searched for publications from 2010 through 2025; the final search was run on January 15, 2026. Forty-eight studies (11 clinical/in vivo and 37 in vitro) assessing photogrammetry in full-arch scenarios (≥4 implants) were included. Primary outcomes were linear, angular, and 3D deviations. Risk of bias was assessed with QUADAS-2 or setting-specific modifications, and certainty was assessed by outcome domain using GRADE. Owing to methodological heterogeneity, a qualitative synthesis and risk-of-bias-stratified robustness analysis were performed.

Results: Forty-eight studies were included. Overall risk of bias was low in 3 studies (6.3%), raised some concerns in 37 (77.1%), and was high in 8 (16.7%). The seven formal GRADE outcome domains were rated moderate (n = 1), low (n = 3), or very low certainty (n = 3). The only moderate-certainty domain—clinical precision of photogrammetry versus IOS—was based on correlated endpoints from one 19-participant cross-over study, which reported lower mean 3D spatial-fit deviation with photogrammetry (7 ± 5 µm) than IOS (61 ± 54 µm). Laboratory trueness and precision findings were mixed and protocol-dependent.

Conclusion: Photogrammetry may provide a precision advantage in selected complete-arch workflows, but the evidence does not establish consistent clinical superiority over IOS or conventional impressions. Confidence is limited by the predominance of studies with methodological concerns, indirect laboratory evidence, protocol heterogeneity, and reliance on single studies for several outcome claims. Device- and protocol-specific verification remains necessary pending independent clinical comparisons linked to prosthesis-level outcomes.

Keywords: Photogrammetry; Dental implants; Dental impression technique; Edentulous mouth; Dental prosthesis; Implant-supported.

Please cite this Article as:
Mokhtari A, Mirzaei A, Ghaffarian Hosseini A, Mirmortazav A. Accuracy of Photogrammetry in Full-Arch Implant Rehabilitation: A Systematic Review. J Craniomaxillofac Res 2026; 13(3): 289-310. DOI: 10.18502/jcr.v13i3.23103

Copyright © 2026 Tehran University of Medical Sciences.
This work is licensed under a Creative Commons Attribution-NonCommercial 4.0 International license (https://creativecommons.org/licenses/by-nc/4.0/). Non-commercial uses of the work are permitted, provided the original work is properly cited.

Introduction

Accurate transfer of implant positions is a prerequisite for predictable full-arch rehabilitation because small positional errors can propagate into framework misfit and downstream complications [1]. Even with modern digital workflows, complete-arch implant scanning remains one of the least forgiving steps, especially as inter-implant span increases and the arch becomes fully edentulous [2]. Clinical workflows therefore still face a practical dilemma: the convenience of direct digital capture versus the risk of cumulative distortion across long-span implant scans [3]. This matters most in full-arch cases, where treatment success depends on coordinating prosthetic fit, passive seating, and occlusal stability in a single superstructure [4].

Conventional open-tray impressions remain a widely used benchmark, yet digital approaches are increasingly preferred for efficiency and patient experience [5]. Photogrammetry was introduced in implant dentistry as a technique that captures the spatial positions of implants by analyzing overlapping calibrated images to reconstruct their 3-dimensional geometry, avoiding the cumulative stitching errors inherent in continuous surface scanning [6]. Recent vitro comparisons show that photogrammetry and IOS can both perform well, but the direction and magnitude of differences depend heavily on the tested system and protocol [7]. In a controlled comparison of edentulous full-arch implant impressions, stereophotogrammetry was evaluated alongside IOS (with and without splinting) and conventional impressions, highlighting protocol-sensitive performance differences across methods [2].

Because photogrammetry is not a single uniform technique, accuracy is influenced by device design and how markers are detected, oriented, and referenced during capture [8]. Even seemingly minor settings can matter; for example, implant reference selection has been shown to change measured trueness outcomes in photogrammetry workflows [9]. Similarly, capture strategy can affect results, and merging two partial photogrammetry scans has been reported to produce different discrepancies than recording in a single scan [10]. From the IOS side, accuracy can degrade with factors like scanning geometry and acquisition conditions, including scanning distance, which has been quantified as a measurable contributor to error [10]. Clinical evidence is now emerging beyond benchtop models, including prospective comparisons where intraoral photogrammetry workflows were assessed against conventional references in complete-arch implant cases [11]. Other clinical work has focused on repeatability, reporting precision outcomes for stereophotogrammetry in full-arch implant recordings under real patient conditions [11]. Several studies have also directly compared intraoral vs extraoral photogrammetry systems, and contrasted them with splinting techniques, reinforcing that "photogrammetry" is not one interchangeable category across devices or workflows [13-16]. Taken together, this growing but heterogeneous evidence base creates a clear need to synthesize accuracy outcomes by system type, protocol variables, and clinical versus in vitro setting. Accordingly, this systematic review aimed to evaluate the accuracy of photogrammetry for complete-arch implant rehabilitation by summarizing trueness and precision outcomes and comparing them with IOS and conventional impression approaches when available..

Materials and Methods

Eligibility criteria

Studies were eligible if they evaluated the accuracy of photogrammetry-based implant position capture in complete-arch implant rehabilitation. The population included edentulous patients or experimental models representing fully edentulous arches rehabilitated with complete-arch implant-supported fixed prostheses (typically ≥ 4 implants). The index test was photogrammetry or stereophotogrammetry-based implant position capture, including extraoral and intraoral photogrammetry workflows. Eligible comparators were intraoral scanning (with or without splinting) and/or conventional open-tray impression techniques. Primary outcomes were measures of accuracy, defined as trueness and/or precision of implant position transfer, reported using linear deviation, root mean square (RMS), ΔEUC, and/or angular deviation. Secondary outcomes, when reported, included workflow efficiency (e.g., capture or scanning time) and clinical feasibility. Both in vivo and in vitro study designs were eligible. Only studies published in English were considered, as resources for accurate translation of highly technical accuracy metrics were not available. No restrictions were applied regarding clinical setting or duration of follow-up.

Information sources

Eligible publication years were January 1, 2010 through December 31, 2025, representing the modern era of digital implant impression workflows. The final database searches were executed on January 15, 2026.

DOI: 10.18502/jcr.v13i3.23103

Search strategy

The search strategy combined terms related to photogrammetry (including device-specific keywords), complete-arch/edentulous implant rehabilitation, and accuracy outcomes (trueness, precision, deviation, RMS). The exact database-specific search strings and the number of records retrieved from each source are reported below.

PubMed (71 hits):

((photogrammetry [Title/Abstract]) OR ("photogrammetric technique" [Title/Abstract]) OR ("photo-grammetry" [Title/Abstract]) OR ("optical triangulation" [Title/Abstract]) OR ("stereo photogrammetry" [Title/Abstract]) OR ("implant photogrammetry" [Title/Abstract]) OR ("PIC system" [Title/Abstract]) OR ("iCam" [Title/Abstract]) OR ("iCam4D" [Title/Abstract]) OR ("PIC dental" [Title/Abstract])) AND (("full arch" [Title/Abstract]) OR ("complete arch"[Title/Abstract]) OR ("edentulous" [Title/Abstract]) OR ("multiple implants" [Title/Abstract]) OR ("implant impression" [Title/Abstract]) OR ("implant scan" [Title/Abstract])) AND (accuracy [Title/Abstract] OR trueness[Title/Abstract] OR precision [Title/Abstract] OR deviation [Title/Abstract] OR "linear deviation"[Title/Abstract] OR "angular deviation" [Title/Abstract] OR "RMS" [Title/Abstract]) AND ("2010/01/01" [Date - Publication]: "3000" [Date-Publication]).

Web of Science (75 hits):

TS = (photogrammetry OR "photogrammetric technique" OR "photo-grammetry" OR "stereophotogrammetry" OR "implant photogrammetry" OR "PIC system" OR iCam OR iCam4D OR "photogrammetric scan") AND TS = ("full arch" OR "complete arch" OR edentulous OR "multiple implants" OR "implant scan" OR "implant impression") AND TS = (accuracy OR trueness OR precision OR deviation OR "linear deviation" OR "angular deviation" OR RMS) AND PY = 2010-2026.

Scopus (75 hits):

TITLE-ABS-KEY (photogrammetry OR "photogrammetric technique" OR "photo-grammetry" OR "stereo photogrammetry" OR "implant photogrammetry" OR "PIC system" OR iCam OR iCam4D OR "photogrammetric scan") AND TITLE-ABS-KEY ("full arch" OR "complete arch" OR edentulous OR "multiple implants" OR "implant scan" OR "implant impression") AND TITLE-ABS-KEY (accuracy OR trueness OR precision OR deviation OR "linear deviation" OR "angular deviation" OR rms) AND (PUBYEAR > 2009).

Embase (73 hits):

(photogrammetry OR 'photogrammetric technique' OR 'photo-grammetry' OR 'stereo photogrammetry' OR 'implant photogrammetry' OR 'photogrammetric scan' OR 'pic system' OR icam OR icam4d) AND ('full arch' OR 'complete arch' OR edentulous OR 'multiple implants' OR 'implant scan' OR 'implant impression') AND (accuracy OR trueness OR precision OR deviation OR 'linear deviation' OR 'angular deviation' OR rms) AND [2010-2026]/py.

Selection process

All retrieved records were imported into reference management software, and duplicates were removed prior to screening. Two reviewers independently screened titles and abstracts for eligibility. Studies deemed potentially eligible by either reviewer underwent full-text assessment. Full-text screening was performed independently by the same two reviewers. Disagreements at any stage were resolved through discussion and consensus. No automation tools were used in the selection process. Only English-language studies were assessed for eligibility.

Data collection process

Data extraction was performed independently by two reviewers using a predefined and standardized extraction sheet in Microsoft Excel. Extracted data were cross-checked for accuracy and completeness, and discrepancies were resolved by consensus. When multiple reports referred to the same study, data were collated and treated as a single study. Study authors were not contacted for missing or unclear information.

Data items (outcomes)

The primary outcomes extracted were measures of accuracy of implant position transfer, including trueness and/or precision. Accuracy metrics included RMS deviation, linear deviation (μm), ΔEUC, and angular deviation (degrees), as reported by the original studies. Secondary outcomes, when available, included workflow efficiency (e.g., acquisition or scanning time) and indicators of clinical feasibility. Most accuracy outcomes were reported as single-time measurements per study; therefore, time-point selection was not applicable.

Data items (other variables)

The following variables were extracted for each includ-

ed study: study identifier, country, study type (in vivo or in vitro), study design, sample (arches/models/patients), arch evaluated (maxillary/mandibular/both), number of implants per arch, photogrammetry system (brand/model), reference method (gold standard), comparator method, accuracy outcome type, accuracy metric, threshold definition (if any), key numeric results, measurement protocol, and operator blinding. If information was missing or unclear, it was recorded as not reported (NR), and no assumptions were made.

Risk of bias assessment

Risk of bias was assessed independently by two reviewers. QUADAS-2 was used for most studies. Modified QUADAS-2 versions were applied for in vitro studies and, where applicable, for clinical studies to ensure the signaling questions and applicability judgments aligned with the study setting while retaining the four standard QUADAS-2 domains (patient/model selection, index test, reference standard, and flow and timing). An overall risk of bias judgment was assigned for each study based on the domain-level assessments. Disagreements were resolved by consensus. Modifications for in-vitro studies involved adapting the patient selection domain to model selection and removing signaling questions related to clinical follow-up, while preserving the intent and structure of all four QUADAS-2 domains.

Effect measures

For accuracy outcomes, effect measures were extracted and reported using the units and definitions provided by the original studies, including linear deviations (μm), RMS values, ΔEUC, and angular deviations (degrees). For precision outcomes, repeatability or variability measures were extracted as reported. No standardized effect size conversion was performed.

Synthesis methods

All studies meeting the eligibility criteria were included in the qualitative synthesis. Data were organized by outcome domain and study type (clinical/in vivo vs in vitro). No unit conversions or statistical transformations were performed. Meta-analysis was not undertaken because study designs, reference standards, photogrammetry systems, comparators, and outcome metrics were too heterogeneous. A qualitative robustness analysis stratified the direction and applicability of findings by overall risk-of-bias category; no quantitative sensitivity meta-analysis was possible.

Reporting bias assessment

Reporting bias was assessed qualitatively by examining completeness of outcome reporting and consistency between stated objectives and reported results across studies. No statistical reporting-bias tests were performed because meta-analysis was not conducted.

Certainty assessment

Certainty was assessed at the outcome-domain level using GRADE domains: risk of bias, inconsistency, indirectness, imprecision, and other considerations. A separate study-outcome traceability appendix was reconciled against every included full text; this appendix contains 52 assessment rows across 48 studies because some studies contribute more than one outcome. Neither assessment-row counts nor overlapping study counts were treated as independent bodies of evidence. Two reviewers independently completed the assessments and resolved disagreements by consensus.

Results

Study selection

Across four databases, 294 records were identified. After removing 180 duplicates, 114 titles/abstracts were screened. Fifty-two reports were sought for retrieval; 2 were not retrieved. Fifty unique full texts were assessed. Two were excluded after full-text review (no experimental photogrammetry index test, n = 1; no quantitative eligible accuracy/trueness/precision/misfit outcome, n = 1), leaving 48 studies for qualitative synthesis (Figure 1). Full-text reconciliation added Prott et al. (2025), which had been marked Include in the Screening workbook but omitted from the original extraction, RoB, GRADE, and manuscript tables. Clinical/in vivo evaluations (n = 11) were reported by Yan et al. [17], Santamaría-Laorden et al. [17], Revilla-León et al. [9,19], Eldabe et al. [19], Fu et al. [21], Zhang et al. [22], Orejas-Pérez et al. [23], Wang et al. [24], Negreiros et al. [25], and Estibalez-Recasens et al. [12]. The remaining studies were in vitro (n = 36), comprising comparative accuracy investigations in models/casts and simulated clinical conditions.

Study characteristics

Across the 48 included studies, 37 were in vitro and 11 were clinical/in vivo. Reported settings included China, Spain, the USA, Portugal, Lebanon, Egypt, Serbia, Thailand, and Türkiye, with several studies reporting multi-country collaborations or NR for country [2,16,18,27].

DOI: 10.18502/jcr.v13i3.23103

Samples commonly involved edentulous arches/models/casts with multiple implants and multi-unit abutments, alongside patient-based clinical evaluations [5,11,17,25]. Photogrammetry approaches included iCam4D systems, PIC camera/system-based extraoral photogrammetry, smartphone/app-based workflows, and intraoral photogrammetry integrated into scanner platforms (e.g., Elite/Aoralscan Elite), with additional prototype/image-guided workflows also evaluated [11,18,28,29]. Reference methods (gold standards) included coordinate measuring machine (CMM) approaches and high-resolution laboratory/industrial scanning, alongside study-specific reference STL workflows depending on design [26,28,30,31]. Comparators included intraoral scanning, conventional impressions, and alternative digitizing workflows; outcomes were typically reported as trueness and/or precision using RMS 3D deviation (μm or mm), linear/Euclidean distance discrepancies, and angular deviations (degrees [2,21,32,33].

Synthesis of results

Trueness (RMS/3D deviation or equivalent)

Trueness was commonly reported using study-defined endpoints such as RMS 3D deviation (μm or mm) and/or deviations between test and reference datasets (complete-arch or scan-body/abutment level), according to each protocol [2,5,11,17]. Trueness results were reported for photogrammetry systems and comparators (e.g., IOS and/or conventional methods) using study-defined reference datasets and endpoints. Yan et al. [17] reported: "SPG vs LS: range 2.70–92.80 μm; median 17.00 μm (Q1 11.68, Q3 22.50)". Cheng et al. reported (2): "SPG: trueness 69.2 (56.0, 75.0) μm; precision 41.1 (22.0, 45.9) μm." Lyu et al. [32] reported: "PG—RMS 38.07 ± 1.71 μm; linear 72.35 ± 16.17 μm; angular 0.25 ± 0.02°."

Precision (repeatability)

Precision was reported as within-method variability across repeated acquisitions, using endpoints such as RMS 3D deviation and/or linear and angular dispersion measures, as defined in each study [2,11,27,13]. Precision outcomes were reported for photogrammetry and comparator workflows using repeated acquisitions or repeated measurements, as defined in each study [25,12,27,31]. Fu et al. reported: "EPG: Trueness (RMS) 31.72 ± 0.59 μm; Precision (RMS) 2.30 ± 1.31 μm" [11]. Tohme et al. reported: "Precision—RMS 3D deviation 0.014 ± 0.013 mm (14 μm)" [27].

Linear/angular discrepancy (μm/mm/degrees) and other explicit endpoints. Linear discrepancy (μm/mm/distance) and angular discrepancy (degrees) were frequently reported alongside RMS-based endpoints, typically as deviations between implant/abutment positions (or inter-implant distances/angles) in test versus reference datasets [18,32,14,34]. Several studies reported accuracy outcomes under different acquisition conditions (e.g., ambient lighting, scanning distance, reference/marker configuration) and/or proportions meeting prespecified deviation thresholds [10,34-36]. Santamaría-Laorden et al. reported: "Overall absolute difference PIC app vs PIC system: 21 ±16 μm and 0.20 ±0.17°; median 17 μm [p25 8, p75 30] and 0.15° [p25 0.07, p75 0.28]." [17]. Jiranaphawiboon et al. reported: "One-phase PG mean ± SD: X 20 ± 4 μm; Y 24 ± 13 μm; Z 8 ± 5 μm; YZ angle 0.023 ± 0.011°; ZX angle 0.033 ± 0.018°; overall RMS 17 ± 10 μm." [14]. Gómez-Polo et al. reported: "Linear trueness (mean, mm): 100 lux 0.027; 500 lux 0.023; 1000 lux 0.025; 5000 lux 0.024; 10 000 lux 0.019." [35]. Benabdallah-M'Rabat et al. reported: "Overall (all 3600 distances): mean absolute distance difference 54 ±46 μm, with 77.08% ≤ 75 μm." [34].

Risk of bias within studies

Risk of bias was evaluated for all 48 studies using QUADAS-2 or setting-specific modified QUADAS-2 criteria. Prott et al. (2025), added during reconciliation, was judged to raise some concerns because it used one in-vitro model and one photogrammetry system, although the index test, reference standard, and flow/timing domains were otherwise judged low risk. Overall, 37/48 studies (77.1%) raised some concerns, 8/48 (16.7%) were at high risk of bias, and only 3/48 (6.3%) were at low risk of bias. The three low-risk studies were Fu et al. (2025), Revilla-León et al. (2025; comparison of photogrammetry systems), and Pinto et al. (2024); all were in vitro. Thus, no low-risk clinical study was available to establish patient-level or prosthesis-level superiority. The eight high-risk studies included several clinically prominent reports. Their results were retained for completeness but were not allowed to drive a confident clinical recommendation. A large subset remained in the "some concerns" category, including Santamaría-Laorden et al. (2025), Ke et al. (2024), Cheng et al. (2024), and Zhou et al. (2024), where at least one domain typically lacked enough detail to support a low-risk judgment. Across domains, the most frequent limitations were observed in patient/model selection and the index test domain. Specifically, patient/model selection was rated some concerns in 32

studies, low in 11, and high in 4, while the index test domain was rated some concerns in 40 studies and low in 7. By comparison, the reference standard domain was more often judged favorable (rated low in 41 studies), with fewer studies rated high [4] or some concerns [2]. Likewise, flow & timing was rated low in 46 studies and high in 1 study.

Findings stratified by risk of bias and robustness

Low-risk stratum (n = 3): all evidence was laboratory-based. These studies supported high repeatability or small deviations for particular photogrammetry workflows, but they did not test clinical outcomes or establish general superiority across devices. Some-concerns stratum (n = 37): this stratum supplied most of the evidence and showed mixed, protocol-dependent directions of effect. Photogrammetry outperformed IOS or conventional impressions in some comparisons, whereas other studies found comparable or less favorable trueness. Prott et al. added favorable trueness for one photogrammetry device but no significant between-group precision difference (P = .192). High-risk stratum (n = 8): several favorable clinical signals, including the within-patient precision comparison, arose in this stratum and were interpreted cautiously. Restricting the synthesis to the three low-risk studies leaves an exclusively laboratory evidence base. Therefore, a conclusion that photogrammetry is clinically superior is not robust to risk-of-bias restriction.

Grade

Formal GRADE assessment comprised seven outcome domains (Table 3): one moderate-certainty domain, three low-certainty domains, and three very-low-certainty domains. The moderate-certainty clinical precision domain was informed by one 19-participant cross-over study; its spatial-fit, cross-arch, and virtual Sheffield measurements are correlated endpoints rather than independent replications. The reconciled study-outcome appendix contains 52 traceability rows across all 48 included studies (13 moderate, 37 low, and 2 very low), but these row counts are not formal pooled GRADE conclusions.

Table 1. Characteristics and key findings of the 48 included studies.

Study	*Implants per arch*	*PG*	*Comp*	*Key numeric results (exact)*
Yan 2023 (16)	*4, 6, or 8*	*iCam4D*	*IOS*	*SPG vs LS: range 2.70–92.80 μm; median 17.00 μm (Q1 11.68, Q3 22.50); IOS vs LS: range 21.30–815.60 μm; median 48.95 μm (Q1 34.78, Q3 75.88); SPG showed lower deviations than IOS; the between-method difference was statistically significant (P<.001); Maxilla vs mandible IOS median 49.25 vs 45.95 μm (P = .403); weak positive correlation between implant number and deviation (r=0.307, P=.008)*
Fu 2025 (10)	*6*	*iCam-4D+A-oralscan Elite*	*IOS*	*EPG: Trueness (RMS) 31.72 ± 0.59 μm; Precision (RMS) 2.30 ± 1.31 μm; Distance deviation 55.55 ± 37.82 μm; Angle deviation 0.36° ± 0.24°; Scanning time 57.40 ± 5.19 s; IOS: Trueness 39.93 ± 7.98 μm; Precision 33.38 ± 13.95 μm; Distance deviation 62.97 ± 50.60 μm; Angle deviation 0.40° ± 0.28°; Scanning time 91.10 ± 20.31 s; IOSA: Trueness 50.60 ± 12.46 μm; Precision 28.35 ± 11.48 μm; Distance deviation 93.37 ± 72.15 μm; Angle deviation 0.32° ± 0.24°; Scanning time 125.00 ± 18.74 s; IPG: Trueness 26.37 ± 1.02 μm; Precision 4.12 ± 0.87 μm; Distance deviation 28.59 ± 24.75 μm; Angle deviation 0.39° ± 0.29°; Scanning time 50.30 ± 6.77 s*
Santamaría-Laorden 2025 (16)	*6*	*PIC app+smartphone*	*PG*	*Overall absolute difference PIC app vs PIC system: 21 ±16 μm and 0.20 ±0.17°; median 17 μm [p25 8, p75 30] and 0.15° [p25 0.07, p75 0.28]. No significant effect of interimplant distance on linear (P>.05) or angular trueness (P>.05). Arch type significantly affected linear trueness (greater deviation in maxilla, P<.001), but not angular trueness (P=.310).*
Revilla-León 2025 (14)	*6*	*PIC system+i-Cam-4D+A-oralscan Elite*	*IOS*	*Linear (mean ± SD): PIC 17 ±4 μm; Icam4D 18 ±6 μm; Grammee 28 ±9 μm; OxoFit 30 ±14 μm; Elite 27 ±5 μm. Angular (mean ± SD): PIC 0.34 ±0.01°; Icam4D 0.29 ±0.05°; Grammee 0.17 ±1.0°; OxoFit 0.31 ±0.02°; Elite 0.27 ±0.02°*

DOI: 10.18502/jcr.v13i3.23103

Study	Implants per arch	PG	Comp	Key numeric results (exact)
Revilla-León 2025 (clinical PG vs splinting) (9)	4	Aoralscan Elite+-Grammee+MicronMapper	IOS+splint	Overall mean ± SD discrepancies (Table 1): Grammee 20 ±9 μm, 0.45 ±0.05°; MicronMapper 20 ±5 μm, 0.18 ±0.02°; Elite 33 ±3 μm, 0.12 ±0.01°; IOConnect 48 ±17 μm, 0.33 ±0.09°. One-way ANOVA: significant differences in linear trueness (F = 26.5, P<.001) and angular trueness (F = 173, P < .001). Grammee and MicronMapper showed the lowest mean linear discrepancies; Elite showed the lowest mean angular discrepancy; MicronMapper and Elite showed the lowest dispersion for angular precision (as reported).
Pinto 2024 (25)	4 and 6	PIC	IOS	Repeatability mean (95% CI): GOM 4 implants 1.07 μm (0.86; 1.29), 6 implants 1.36 μm (1.08; 1.65); D2000 4 implants 2.05 μm (1.89; 2.21), 6 implants 3.17 μm (3.01; 3.33); S900 Arti 4 implants 3.61 μm (3.23; 3.99), 6 implants 2.15 μm (2.04; 2.25); iCam 4 implants 7.01 μm (6.11; 7.91), 6 implants 8.67 μm (8.06; 9.28); PIC 4 implants 5.18 μm (4.60; 5.76), 6 implants 13.88 μm (12.62; 15.14); TRIOS 3 4 implants 20.52 μm (18.33; 22.72), 6 implants 40.32 μm (36.29; 44.36) with 28.79% >50 μm; iTero 4 implants 20.5 μm (17.37; 23.63), 6 implants 38.86 μm (34.01; 43.71) with 27.28% >50 μm
Ke 2024 (34)	6	iCam4D	IOS	SSLS: overall linear trueness median (IQR) 6.6 (2.0) μm; linear precision 5.7 (6.4) μm; mucosal trueness 33.4 (16.9) μm; mucosal precision 21.6 (7.4) μm. PG (ICam4D): overall linear trueness 58.4 (3.1) μm; precision 6.8 (6.0) μm; span medians D12 39.2 μm, D13 99.7 μm, D14 69.8 μm, D15 9.1 μm, D16 74.8 μm. IOS (Aoralscan 3): overall linear trueness 214.6 (96.0) μm; precision 329.1 (328.8) μm; span medians D12 131.9 μm, D13 169.2 μm, D14 183.3 μm, D15 206.4 μm, D16 296.5 μm; mucosal trueness 59.8 (21.6) μm; mucosal precision 70.4 (46.1) μm.
Cheng 2024 (2)	6	PIC	IOS+splint+CNV	CI: Overall RMS 3D trueness 87.3 (75.8, 120.9) μm; precision 77.1 (58.8, 102.6) μm. IOS: trueness 79.6 (72.3, 102.4) μm; precision 59.2 (46.9, 94.6) μm. MIOS: trueness 89.5 (61.5, 99.5) μm; precision 73.4 (46.8, 126.1) μm. SPG: trueness 69.2 (56.0, 75.0) μm; precision 41.1 (22.0, 45.9) μm. Site-specific trueness RMS 3D (μm): CI—#12 51.10; #10 89.50; #7 92.65; #5 88.40; #3 116.30. IOS—#12 50.40; #10 90.95; #7 112.75; #5 69.75; #3 85.10. MIOS—#12 28.30; #10 86.45; #7 114.40; #5 112.10; #3 103.60. SPG—#12 37.15; #10 97.30; #7 71.95; #5 61.70; #3 75.40. Angular deviations lowest in SPG and mostly <0.4°, CI and IOS exceeded 0.4°.
Zhou 2024 (35)	4 or 6	iCam4D	IOS	PG: Overall distance deviation 145 ±196 μm (median 69 μm, IQR 145); 69.7% of deviations <150 μm. Overall angle deviation 0.82 ±0.88° (median 0.65°, IQR 0.91). CNV: Overall distance deviation 96 ±150 μm (also reported mean 47 μm, SD 39; median 38 μm, IQR 41). Overall angle deviation 0.74 ±0.62° (median 0.59°, IQR 0.81). PG distance deviations significantly larger than CNV (P < 0.001); angular deviations not significantly different (P = 0.267). Correlations—PG: inter-implant distance vs distance r = −0.145 (P = 0.028), vs angle r = −0.198 (P=0.003); inter-implant angulation vs distance r = 0.205 (P = 0.002), vs angle r = 0.172 (P = 0.009). CNV: inter-implant distance vs distance r = 0.347 (P < 0.001); no significant correlations for angle.
Tohme 2021 (12)	4	PIC	IOS	DIOS: Trueness—angular deviation 1.744 ± 0.175°; RMS 3D deviation 0.536 ± 0.063 mm (536 μm). Precision—RMS 3D deviation 0.039 ± 0.009 mm (39 μm); angular precision not significantly different from DPG (p = 0.067; exact mean NR). DPG: Trueness—angular deviation 0.724 ± 0.064°; RMS 3D deviation 0.078 ± 0.001 mm (78 μm), significantly lower than DIOS (p < 0.001). Precision—RMS 3D deviation 0.014 ± 0.013 mm (14 μm), significantly better than DIOS (p < 0.001); angular precision not significantly different from DIOS (p = 0.067; exact mean NR).

Study	Implants per arch	PG	Comp	Key numeric results (exact)
Eldabe 2025 (18)	4	PIC system	IOS+CNV	IOS: Overall (52 implants) ΔEUC mean 59.8 μm (SD 30; range 8–143 μm); ΔANGLE mean 1.4° (SD 0.44; range 0.67–2.9°); both significantly higher than IPS (P<.001). IPS: Overall ΔEUC mean 30.7 μm (SD 18; range 0–107 μm); ΔANGLE mean 0.78° (SD 0.27; range 0.24–1.4°); ΔEUC significantly <100 μm and ΔANGLE significantly <1°; paired comparison vs IOS significant (P<.001; 95% CI for ΔEUC difference −40.33 to −17.88; for ΔANGLE −0.8 to −0.53). By arch: IOS Euclidian mean 48.7–75.5 μm; angular mean 1.1–2.0°. IPS Euclidian mean 25.0–39.3 μm; angular mean 0.62–0.92°.
Brakoč 2025 (36)	4	iCam4D	IOS	IPG (Aoralscan Elite IPG) mean ranks (Kruskal–Wallis): distance SD 17.67; integrated distance 19.20; integrated absolute distance 17.13 (lowest mean ranks for the reported metrics); IPG differed significantly from TRIOS 5, Medit i700, and Aoralscan 3 for all three metrics (all p<0.01). TRIOS 5 mean ranks: distance SD 54.65; integrated distance 52.30; integrated absolute distance 70.75. Medit i700 mean ranks: distance SD 89.52; integrated distance 65.62; integrated absolute distance 67.28. Aoralscan 3 mean ranks: distance SD 80.17; integrated distance 104.88; integrated absolute distance 86.83 (worst integrated metrics).
Fu 2024 (20)	4–6	iCam4D	IOS+CNV	IOS: Distance deviations median 75 μm (Q25–Q75: 31–138 μm; n=248 distances); angle deviations median 0.40° (0.19–0.80°; n=248); RMS errors median 69 μm (57–94 μm; n=22). SPG: Distance deviations median 60 μm (28–109 μm); angle deviations median 0.31° (0.14–0.56°); RMS errors median 45 μm (36–52 μm). Distance deviations not significantly different between IOS and SPG (p=0.15); IOS angle deviations and RMS significantly higher than SPG (p<0.01). All median distance deviations <150 μm.
Jiranaphawiboon 2025 (13)	6	PIC	PG	One-phase PG mean ± SD: X 20 ± 4 μm; Y 24 ± 13 μm; Z 8 ± 5 μm; YZ angle 0.023 ± 0.011°; ZX angle 0.033 ± 0.018°; overall RMS 17 ± 10 μm. Two-phase PG mean ± SD: X 23 ± 8 μm; Y 22 ± 9 μm; Z 10 ± 5 μm; YZ angle 0.027 ± 0.014°; ZX angle 0.031 ± 0.010°; overall RMS 18 ± 9 μm. No significant differences between protocols (p>0.05).
Zhang 2023 (21)	4–7	PIC	CNV	Overall mean ±SD distance deviation 70 ±57 μm (95% CI 56–84), significantly less than 150 μm (P<.001); overall mean ±SD angular deviation 0.432 ±0.348° (95% CI 0.346–0.518). At implant level, 90.8% of distance deviations <150 μm (95% CI 83.7–97.8); at patient level, 71.4% of jaws had maximum distance deviation <150 μm (95% CI 47.8–95.1). Distance deviations correlated positively with inter-implant distance (r = 0.371, P=.002), with significantly higher deviations for distances 40–50 mm vs 30–40 mm (P=.012) and for > 40 mm vs ≤40 mm (P<.001); inter-implant angulation and jaw had no significant effect.
Lyu 2025 (30)	6	PIC	IOS+CNV	Complete-arch range (abcdef) trueness (mean ± SD): CNV—RMS 34.55 ± 7.28 μm; linear 47.78 ± 41.98 μm; angular 0.22 ± 0.04°. IOS—RMS 68.49 ± 22.27 μm; linear 120.47 ± 62.88 μm; angular 0.31 ± 0.06°. PG—RMS 38.07 ± 1.71 μm; linear 72.35 ± 16.17 μm; angular 0.25 ± 0.02°. Precision for abcdef (median, IQR): CNV—RMS 8.82 (10.39) μm; linear 26.50 (44.54) μm; angular 0.05 (0.05)°. IOS—RMS 23.06 (28.64) μm; linear 63.50 (73.01) μm; angular 0.06 (0.08)°. PG—RMS 1.78 (1.98) μm; linear 10.66 (17.39) μm; angular 0.01 (0.04)°. CNV trueness stable across ranges; IOS trueness decreased significantly with range expansion; CNV and PG significantly more true than IOS at complete arch (p ≤ 0.003).

DOI: 10.18502/jcr.v13i3.23103

Study	Implants per arch	PG	Comp	Key numeric results (exact)
Liu 2024 (37)	4 or 6	PIC	IOS	Overall results across casts (Table 3): OI—Trueness: distance 72 ±60 μm (95% CI 61–83), angle 0.40 ±0.40° (0.33–0.48), RMS 35 ±18 μm (28–48); Precision: distance 73 ±84 μm (66–81), angle 0.33 ±0.50° (0.29–0.38), RMS 36 ±26 μm (32–41). SPG—Trueness: distance 35 ±19 μm (31–39), angle 0.25 ±0.16° (0.22–0.28), RMS 21 ±4 μm (20–23); Precision: distance 10 ±10 μm (9–11), angle 0.07 ±0.08° (0.06–0.08), RMS 9 ±7 μm (8–10). IOS—Trueness: distance 168 ±133 μm (143–193), angle 0.43 ±0.34° (0.37–0.50), RMS 88 ±21 μm (81–96); Precision: distance 100 ±122 μm (89–111), angle 0.29 ±0.26° (0.27–0.31), RMS 57 ±32 μm (51–62). SPG significantly more accurate than OI and IOS for all outcomes (P < .001).
Revilla-León 2025 (registration) (38)	6	PIC	IOS	Lumina: mean ± SD 105 ±23 μm (median 101 ±31; min 67; max 137). TRIOS 5: 123 ±29 μm (median 127 ±29; min 80; max 188). Primescan: 118 ±23 μm (median 116 ±32; min 90; max 162). i700: 127 ±29 μm (median 133 ±41; min 73; max 175). Elite without CHAs: 108 ±31 μm (median 95 ±39; min 67; max 183). Elite with CHAs: 98 ±28 μm (median 101 ±41; min 43; max 137); lowest mean discrepancy; ANOVA P=.044; Tukey: Elite with CHAs vs i700 P=.046
Revilla-León 2025 (1-scan vs 2-scan) (8)	6	iCam4D	IOS	ICam4D 1-scan: linear 19 ±7 μm; angular 0.176 ±0.012°. ICam4D 2-scan: linear 24 ±8 μm; angular 0.163 ±0.026°. Grammee 1-scan: linear 29 ±9 μm; angular 0.145 ±0.074°. Grammee 2-scan: linear 32 ±9 μm; angular 0.294 ±0.127°. OxoFit 1-scan: linear 31 ±16 μm; angular 0.223 ±0.038°. OxoFit 2-scan: linear 31 ±9 μm; angular 0.153 ±0.024°. One-scan protocol showed better linear and angular trueness and angular precision than two-scan for ICam4D (P=.048 linear; P=.022 angular). ICam4D showed the lowest mean linear discrepancies and dispersion values among the tested systems.
Revilla-León 2025 (mandible, in vivo) (18)	4	PIC	IOS	MicronMapper: linear 25 ±17 μm; angular 0.71 ±0.08°. Elite intraoral PG: linear 37 ±12 μm; angular 0.44 ±0.06° (best angular trueness; ANOVA P<.001). IOConnect + TRIOS 5: linear 39 ±6 μm; angular 0.76 ±0.14°; linear trueness differences nonsignificant among groups (ANOVA P=.089); IOConnect showed significantly better linear precision than MicronMapper and Elite (Levene P=.008; pairwise P=.017).
Sallorenzo 2022 (39)	6	PIC	IOS	Parallel cast (PIMP): PiC—linear error 20 μm (P=.031), angular error 0.354° (P=.087), precision SD ±32 μm and ±0.280°; TRIOS 3—linear error 100 μm (P<.001), angular error 1.177° (P<.001), precision SD ±292 μm and ±0.474°. Angled cast (AIMP): PiC—linear error 10 μm (P=.055), angular error 0.084° (P=.045), precision SD ±65 μm and ±0.246°; TRIOS 3—linear error 23 μm (P=.179), angular error 0.529° (P<.001), precision SD ±205 μm and ±0.841°.
Tohme 2023 (31)	4	PIC	IOS+CNV	SPG: trueness—RMS WSB 0.088 ±0.006 mm; RMS FAS 0.213 ±0.064 mm; angular deviation 0.809 ±0.005°; precision—RMS WSB 0.002 ±0.001 mm; RMS FAS 0.002 ±0.003 mm; angular deviation 0.010 ±0.011°. IOS (TRIOS 3): trueness—RMS WSB 0.148 ±0.061 mm; RMS FAS 0.112 ±0.032 mm; angular deviation 1.081 ±0.348°; precision—RMS WSB 0.063 ±0.035 mm; RMS FAS 0.067 ±0.030 mm; angular deviation 0.221 ±0.088°. Conventional impression: trueness—RMS WSB 0.115 ±0.037 mm; RMS FAS 0.166 ±0.038 mm; angular deviation 0.922 ±0.194°; precision—RMS WSB 0.103 ±0.024 mm; RMS FAS 0.166 ±0.033 mm; angular deviation 1.142 ±0.296°. SPG showed significantly superior trueness and precision for WSB RMS and angular deviation compared with IOS and conventional methods (P<.001).

Study	Implants per arch	PG	Comp	Key numeric results (exact)
Revilla-León 2021 (26)	6	PIC	IOS+CNV	CNV: median 3D discrepancy 11.7; x 7.3, y 8.9, z 1.8; angular XZ 0.1°, YZ −0.1° (lowest overall discrepancy). PG (Icam4D): median 3D discrepancy 77.6; x 23.8, y 73.7, z −4.7; angular XZ 0.1°, YZ 0.3° (significantly higher y-axis and 3D gap than all others, P=.004). IOS-1 (iTero): median 3D discrepancy 18.4; x 4.1, y 17.5, z −4.1; angular XZ −0.1°, YZ −0.1°. IOS-2 (TRIOS 3): median 3D discrepancy 21.1; x 9.7, y 18.0, z −4.9; angular XZ −0.2°, YZ 0.2°.
Abuduwaili 2025 (5)	6	iCam4D	IOS+CNV	CON trueness medians: 3D 66.05 μm; X 32.79 μm; Y 42.28 μm; Z 13.54 μm; angular 0.35°; RMS 40.50 μm. CON precision medians: 3D 39.32 μm; angular 0.24°; RMS 36.55 μm. IOS trueness medians: 3D 78.58 μm; X 41.60 μm; Y 49.93 μm; Z 16.65 μm; angular 0.52°; RMS 91.75 μm. IOS precision medians: 3D 45.33 μm; angular 0.38°; RMS 82.8 μm. PG-1 (Icam4D) trueness medians: 3D 25.23 μm; X 12.59 μm; Y 13.56 μm; Z 7.91 μm; angular 0.12°; RMS 10.87 μm. PG-1 precision medians: 3D 15.80 μm; angular 0.10°; RMS 3.7 μm. PG-2 (PIC) trueness medians: 3D 28.15 μm; X 15.53 μm; Y 17.35 μm; Z 9.18 μm; angular 0.14°; RMS 13.35 μm. PG-2 precision medians: 3D 17.78 μm; angular 0.13°; RMS 4.6 μm.
Santamaría-Laorden 2025 (PIC app vs system) (40)	6	PIC	IOS	PIC system®: linear 18.21 ± 12.21 μm; angular 0.10 ± 0.07°; median [p25, p75] 16.91 [8.00, 26.98] μm and 0.09 [0.05, 0.15]°; min–max 0.01–54.48 μm and <0.01–0.36°. PIC app®: linear 30.92 ± 20.88 μm; angular 0.16 ± 0.09°; median [p25, p75] 29.85 [12.58, 46.60] μm and 0.18 [0.08, 0.24]°; min–max 0.07–87.62 μm and <0.01–0.42°. Mean differences vs PIC system®: +12.70 μm (95% CI 10.47–14.94) and +0.07° (95% CI 0.05–0.07), both P<.001.
Gómez-Polo 2025 (33)	6	Aoralscan Elite	PG	Linear trueness (mean, mm): 100 lux 0.027; 500 lux 0.023; 1000 lux 0.025; 5000 lux 0.024; 10 000 lux 0.019. Angular trueness (mean, °): 100 lux 0.070; 500 lux 0.053; 1000 lux 0.086; 5000 lux 0.054; 10 000 lux 0.046. Statistically significant lower linear deviations at 10 000 lux vs 100 lux (Δ0.008 mm, P=.022) and 1000 lux (Δ0.006 mm, P=.002); significantly lower angular deviations for 500, 5000, 10 000 lux vs 1000 lux (P<.001) and for 10 000 vs 100 lux (P=.009). No significant differences in precision for linear (P=.334) or angular (P=.689) deviations.
Revilla-León 2025 (inter-implant distance) (37)	6	iCam4D	IOS	Overall per-group mean±SD linear discrepancies (μm): Group −2: 33±2; Group 0: 35±5; Group 2: 31±3; Group 4: 39±4 (worst trueness); Group 6: 34±4; Group 8: 33±3. Angular discrepancies (degrees): −2: 0.11±0.02; 0: 0.12±0.02; 2: 0.11±0.02; 4: 0.11±0.02; 6: 0.11±0.02; 8: 0.12±0.02. One-way ANOVA Welch showed significant linear trueness differences among groups (P<.001); Tukey post hoc identified multiple significant pairs, with Group 4 differing from all others; linear precision differed only between Groups −2 and 0 (P=.033). Angular trueness (P=.369) and precision (P=.587) showed no significant differences.
Bin Farrah 2025 (13)	4	iCam4D	PG	CI: RMS 3D mean±SD (μm): 0° 32±8; 10° 32±9; 20° 26±10; global 29±10. Angular deviation (°): 0° 0.12±0.06; 10° 0.21±0.05; 20° 0.16±0.06; global 0.16±0.07. PP (PIC): RMS 3D (μm): 0° 52±5; 10° 44±6; 20° 49±7; global 48±7. Angular (°): 0° 0.56±0.23; 10° 0.48±0.15; 20° 0.79±0.17; global 0.62±0.23. IP (ICam4D): RMS 3D (μm): 0° 50±3; 10° 60±3; 20° 43±3; global 51±8. Angular (°): 0° 0.52±0.11; 10° 0.32±0.03; 20° 0.53±0.03; global 0.46±0.12. CI showed significantly lower 3D and angular deviations than PP and IP across all models (p<0.001).

DOI: 10.18502/jcr.v13i3.23103

Study	Implants per arch	PG	Comp	Key numeric results (exact)
Muslu 2025 (15)	5	PIC	IOS	IOS (no PAD): global RMS trueness 63.08 ± 13.57 μm; ΔAD exceeded 0.4° at all sites (e.g., #13–16 overall 1.10°); precision RMS 11.97 ± 3.24 μm. IOS-C: global RMS trueness 39.13 ± 9.74 μm; ΔAD 0.39–0.60° (several sites >0.4°); precision RMS 11.73 ± 3.15 μm. IOS-LE: global RMS trueness 32.43 ± 4.84 μm; ΔAD 0.33–0.46° (exceeded 0.4° mainly in distal model); precision RMS 11.57 ± 3.36 μm. PG-I (ICam4D): global RMS trueness 18.21 ± 3.27 μm; ΔAD 0.11–0.25° (all <0.4°); precision RMS 8.13 ± 1.46 μm (best). PG-O (OxoCore): global RMS trueness 35.30 ± 8.52 μm (distal model up to 48.19 ± 6.37 μm); ΔAD 0.20–0.55° (exceeded 0.4° mainly in distal model); precision RMS 10.93 ± 2.89 μm.
Bratos 2018 (42)	5	PIC	IOS	Precision (SE of linear measurements): CMM 3.9 μm (95% CI 2.7–7.1); conventional impression 17.2 μm (95% CI 10.3–49.4); photogrammetry grand mean for clinically feasible groups (MinR-AvgO, MinR-MaxO, AvgR-AvgO, MaxR-AvgO) 26.8 μm (95% CI 18.1–51.4). Overall linear measurement error (trueness): CMM average error 4.6 μm (95% CI 3.5–6); conventional method 26.2 μm (95% CI 15.9–36.6); photogrammetry groups accuracy 47–63 μm with grand mean 55.2 μm (95% CI 8.8–130.8). Angular SE smallest for CMM (x 0.013°, y 0.016°); photogrammetry x-angle SE 0.073°–0.229°, y-angle SE 0.222°–0.344°.
Chen 2024 (43)	2, 4, or 6 (test-dependent)	PIC	IOS	Working-range test: optimal distance 200–250 mm with minimum measurement error <0.05 mm; within 150–350 mm, 75% of errors <0.19 mm. Pose experiment (2/4/6 scan bodies): median axial error 0.06/0.09/0.10 mm; median radial error 0.05/0.10/0.11 mm; Q3 angular error 6.94/7.03/7.56×10^{-3} rad (~0.40–0.43°). CT vs IOS vs PG: MAE (mm) TRIOS 4 0.1643, Aoralscan 2 0.1782, RID photogrammetry 0.1056; RMSE (mm) TRIOS 4 0.1885, Aoralscan 2 0.2007, RID photogrammetry 0.0984; time 134 s, 257 s, and 64 s respectively.
Pozzi 2025 (IGP) (44)	4 or 6	PIC	IOS	Overall (all 126 implants): ΔX −0.05 ±29.95 μm (range −75.17 to 68.00; P75 22.00), ΔY 0.01 ±31.65 μm (−68.0 to 93.93; P75 19.18), ΔZ −0.02 ±12.95 μm (−39.0 to 43.51; P75 6.76); ΔEUC 43.02 ±26.24 μm (3.41–190.23; P75 58.21); ΔANGLE 0.43 ±0.22° (0.03–0.86; P75 0.61). Stratified by implant number: 4-implant casts – ΔEUC 38.32 ±20.01 μm (9.04–81.12; P75 54.11), ΔANGLE 0.36 ±0.21° (0.03–0.75; P75 0.48); 6-implant casts – ΔEUC 49.41 ±30.04 μm (3.02–190.22; P75 60.88), ΔANGLE 0.48 ±0.22° (0.04–0.86; P75 0.67); both outcomes significantly higher for 6 vs 4 implants (ΔEUC P=.017; ΔANGLE P=.003). By position in 6-implant casts, ΔEUC did not differ among A,F (posterior), B,E (intermediate), C,D (anterior) (P=.241), but ΔANGLE was significantly higher for anterior (C,D) vs intermediate (B,E) and posterior (A,F) (P=.009); no positional differences were found for 4-implant casts.

Study	Implants per arch	PG	Comp	Key numeric results (exact)
Revilla-León 2024 (scan distance) (10)	6	iCam4D	PG	Overall mean±SD linear discrepancies (μm): 20-cm group 25 ±4; 30-cm group 17 ±4; 35-cm group 27 ±6. Overall mean±SD angular discrepancies (°): 20-cm group 0.15 ±0.01; 30-cm group 0.17 ±0.02; 35-cm group 0.19 ±0.01. One-way ANOVA showed significant differences in linear (F=35.8, P<.001) and angular trueness (F=48.2, P<.001) among groups; Tukey test: linear 20 vs 30 and 30 vs 35 both P<.001; angular 20 vs 30 P=.003, 20 vs 35 P<.001, 30 vs 35 P<.001. Precision (Levene) showed no significant differences for linear (P=.197) or angular (P=.229) measurements.
Bergin 2013 (45)	5	PIC	CNV	Precision (SEm global xyz): CMM 3.9 μm; Photogrammetry 5.6 μm (95% CI 3.4–16.1); Conventional 17.2 μm (95% CI 10.3–49.4). Mean linear error vs CMM: Photogrammetry 28.8 μm (max 57.4 μm); Conventional 26.2 μm (max 51.0 μm). Mean angular error: Photogrammetry X 0.17°, Y 0.24°; Conventional X 0.11°, Y 0.15°. No significant difference in global accuracy between photogrammetry and conventional (P=0.54).
Orejas-Pérez 2022 (22)	8	IOS	IOS	PIC showed highest precision: distances <75 μm in 98.6% (maxilla) and 95.4% (mandible); angulations <0.6° in 100% of cases for both arches. Maximum distance error per segment: 108.2 μm (maxilla) and 104.4 μm (mandible); long span (1–8): 64.5 μm maxilla, 53.2 μm mandible. Trios 3 showed lower precision (distances <75 μm: 77.9% maxilla, 68.2% mandible; max error up to 476.4 μm). True Definition was intermediate (distances <75 μm: 90.4% maxilla, 80.0% mandible; max error up to 342.9 μm). Precision for IOS systems worsened with increasing inter-implant distance, especially in the mandible.
Benabdallah-M'Rabat 2025 (32)	6	PIC	PG	Overall (all 3600 distances): mean absolute distance difference 54 ±46 μm, with 77.08% ≤75 μm. By model: PM 53 ±38 μm, 74.83% ≤75 μm; AM 55 ±54 μm, 79.33% ≤75 μm. By camera: A1 52 ±43 μm, 80.67% ≤75 μm; A2 57 ±49 μm, 73.50% ≤75 μm. By references: 1R 54 ±41 μm, 77.00%; 2R 57 ±57 μm, 77.50%; 3R 51 ±38 μm, 76.75%. Overall angle trueness (1440 angles): 0.341 ±0.301°, 82.08% ≤0.6°. PM 0.397 ±0.322°, 76.25%; AM 0.285 ±0.267°, 87.92%. A1 0.329 ±0.238°, 83.75%; A2 0.353 ±0.353°, 80.42%. References: 1R 0.321 ±0.273°, 89.17%; 2R 0.365 ±0.330°, 79.58%; 3R 0.337 ±0.298°, 77.50%. Distance precision (68 400 repeated distances): mean absolute difference 18 ±23 μm, 84.69% ≤75 μm (PM 80.22%, AM 89.17%; A1 100.00%, A2 87.08%; 1R 100.00%, 2R 97.29%, 3R 88.50%). Angle precision (22 800 repeated angles): 0.048 ±0.074°, 93.54% ≤0.6° (PM 100.00%, AM 87.08%; A1 100.00%, A2 87.08%; 1R 100.00%, 2R 97.29%, 3R 83.33%).
Revilla-León 2025 (framework connection) (46)	6	PIC	PG	PG group (PIC): linear 35 ±7 μm, median ±IQR 38 ±7 μm; angular 0.19 ±0.02°, median 0.18 ±0.03°. TRIOS 4: ISB 61 ±13 μm & 0.47 ±0.12°; SSB 44 ±11 μm & 0.56 ±0.06°; CF 79 ±15 μm & 0.34 ±0.06°. i700: ISB 65 ±19 μm & 0.24 ±0.04°; SSB 81 ±82 μm & 0.31 ±0.09°; CF 27 ±17 μm & 0.14 ±0.08°. iTero: ISB 87 ±32 μm & 0.32 ±0.07°; SSB 75 ±98 μm & 0.31 ±0.06°; CF 25 ±8 μm & 0.12 ±0.04°. CS3800: ISB 157 ±44 μm & 0.34 ±0.13°; SSB 115 ±28 μm & 0.25 ±0.07°; CF 44 ±9 μm & 0.12 ±0.04°. LBS (T710): ISB 43 ±1 μm & 0.27 ±0.01°; SSB 41 ±2 μm & 0.29 ±0.01°; CF 20 ±2 μm & 0.08 ±0.01°. Overall, PG and CF subgroups showed the lowest linear and angular discrepancies, while SSB subgroups had the lowest precision.

DOI: 10.18502/jcr.v13i3.23103

Study	Implants per arch	PG	Comp	Key numeric results (exact)
Revilla-León 2025 (implant reference) (7)	6	PIC	PG	Overall mean±SD discrepancies (Table 2): IPR-3: 24 ±6 μm, 0.13 ±0.01°; IPR-11: 28 ±3 μm, 0.13 ±0.01°; IPR-14: 30 ±6 μm, 0.14 ±0.01°. One-way ANOVA showed significant linear (F=6.51, P=.003) and angular (F=5.30, P=.009) trueness differences; Tukey test found significant differences only between IPR-11 and IPR-14 (P<.001). IPR-3 achieved the "highest trueness" among groups. Levene tests showed no significant precision differences for linear (P=.197) or angular (P=.235) measurements.
Pozzi 2025 (Elite IPG) (27)	4–6	IPG	PG	Overall (146 implants): ΔX −3.97 ± 32.8 μm (range −85.62–71.11; 75th percentile 19.34 μm), ΔY −1.97 ± 25.03 μm (−81.10–56.17; 75th 15.71 μm), ΔZ −33.3 ± 34.77 μm (−136.50–33.39; 75th −0.87 μm). ΔEUC 57.22 ± 27.41 μm (5.50–138.00; 75th 73.73 μm), ΔANGLE 0.26° ± 0.19° (0.01–1.00; 75th 0.33°). Stratified by implant number (Table 2): 4 implants: ΔEUC 55.1 ± 27.7 μm, ΔANGLE 0.27° ± 0.18°; 5 implants: ΔEUC 50.8 ± 22.0 μm, ΔANGLE 0.27° ± 0.20°; 6 implants: ΔEUC 63.9 ± 29.5 μm, ΔANGLE 0.25° ± 0.18°. Mixed models found significant deviations for ΔZ, ΔEUC, ΔANGLE vs reference (p<0.01), and implant number significantly affected only ΔZ (p=0.03).
Wang 2023 (23)	NR			Cumulative RMS deviation = 140.4 μm
Negreiros 2025 (24)	≥4	PIC	IOS	Spatial Fit: PG average 3D deviation 7±5 μm vs IOS 61±54 μm; PG average maximum 3D deviation 18±10 μm vs IOS 152±95 μm. Cross-Arch Distance: PG average deviation 10±1 μm and average maximum 20±15 μm vs IOS 89±6 μm and 181±113 μm. Virtual Sheffield test: PG average terminal-implant deviation 38±31 μm and average maximum 70±41 μm vs IOS 447±420 μm and 807±654 μm. Vertical and horizontal deviations followed the same pattern, with PG showing markedly lower dispersion and maximum errors.
Faria 2025 (precision, CCI) (12)	CCI A: 6; CCI B/C: 4	PIC	IOS	Across all distributions and scanners, mean RMS values were consistently below 30 μm. CCI A (6 implants): Trios 3 12.66 μm, Medit i500 11.36 μm, PIC 11.28 μm; pooled RMS 11.77 μm. CCI B (4 implants): Trios 3 16.96 μm, Medit i500 16.69 μm, PIC 14.44 μm; pooled RMS 16.03 μm (highest RMS, lower precision). CCI C (4 implants): Trios 3 5.96 μm, Medit i500 7.36 μm, PIC 11.54 μm; pooled RMS 8.29 μm (best precision). No statistically significant differences among scanners overall (device-level p=0.097). Implant distribution significantly affected precision, with CCI B showing higher RMS and CCI C the lowest (p<0.001).
Estibalez-Recasens 2025 (11)	6	PIC system	PG	Linear precision: mean±SD 14.71±12.21 μm (range 0–61 μm); no linear discrepancies exceeded 75 μm. Angular precision: mean±SD 0.072±0.064° (range 0–0.345°); no angular discrepancies exceeded 0.6°. Significant differences in precision were observed among different interimplant spans for both linear and angular measurements (Kruskal–Wallis P<.05), with Sidak post-hoc tests identifying multiple significant pairwise differences (e.g., longer spans showed higher discrepancies), but all values remained within predefined clinical thresholds.
Revilla-León 2025 (registration, 4 PG systems) (47)	6	iCam4D	PG	iCam4D: 106 ±28 μm; Grammee: 116 ±52 μm; OxoFit: 103 ±38 μm (lowest mean); Elite intraoral PG: 116 ±21 μm. One-way ANOVA showed no significant differences in trueness among systems (P=.270). Levene test showed no significant differences in precision among systems (P=.130). Overall registration discrepancies across all PG systems ranged from 103 ±38 μm to 116 ±52 μm.

Study	Implants per arch	PG	Comp	Key numeric results (exact)
Revilla-León 2023 (28)	6	PIC	IOS+CNV	Overall accuracy (trueness ± precision) values: CNV group 18.40 ±6.81 mm; PG group 20.15 ±25.41 mm. Significant differences between CNV and PG for linear discrepancies on x axis (U=1380.00, P=.027) and z axis (U=601.00, P<.001), and angular discrepancies in XZ angle (U=869.00, P<.001) and YZ angle (U=788.00, P<.001). Significant 3D discrepancy differences at implant 1 (U=0.00, P<.001), implant 2 (U=0.00, P<.001), implant 3 (U=6.00, P<.001), and implant 6 (U=9.00, P<.001); conventional method showed more uniform 3D discrepancies across implants, photogrammetry showed uneven pattern.
Demirel 2023 (29)	6	iCam4D	IOS	Surface trueness (RMS median, min–max): iCam4D 104 µm (102–111); X5 36 µm (33–51); S7 44.5 µm (35–49); PS 51 µm (46–64); T4 58.5 µm (41–77). Scanner type significantly affected trueness (P<.001); X5 and S7 most accurate; iCam4D least accurate. Surface precision (RMS dispersion median): iCam4D 1.50 µm; X5 2.80 µm; S7 3.90 µm; PS 5.80 µm; T4 12.90 µm (P<.001). Angular trueness (median): iCam4D 0.52°; X5 0.45°; S7 0.52°; PS 0.34° (lowest); T4 0.48° (P=.001). Angular precision not significantly different among scanners (P=.084).
Faria 2025 (trueness, CCI) (48)	CCI A: 6; CCI B/C: 4	PIC	IOS	By implant distribution and scanner (Table 2): Trios 3 – TA (CCI A, 6 implants): median RMS 29.55 µm (IQR 27.85–29.73); TB (CCI B, 4 implants): 58.80 µm (45.78–63.38); TC (CCI C, 4 implants close): 18.75 µm (17.95–20.75), p<0.001, no difference A vs B (p=0.142). Medit i500 – MA: 33.95 µm (32.10–37.20); MB: 24.45 µm (20.48–25.70); MC: 13.65 µm (11.90–15.60), p<0.001, no difference B vs C (p=0.119). PIC Dental photogrammetry – PA: 53.55 µm (53.03–53.95); PB: 49.45 µm (45.38–51.38); PC: 43.70 µm (43.38–45.88), p<0.001, with no differences A vs B (p=0.058) or B vs C (p=0.105). By implant distribution regardless of scanner (Table 3): CCI A median 34.20 µm (IQR 29.70–53.15), CCI B 45.75 µm (24.58–57.05), CCI C 19.00 µm (15.58–43.40), p<0.001, no difference A vs B (p=0.722). By scanner regardless of distribution (Table 4): Trios 3 median 29.20 µm (20.13–51.50); Medit i500 24.45 µm (14.45–32.63); PIC Dental 49.45 µm (44.13–53.30), p<0.001; Medit showed highest trueness, PIC the lowest. All median deviations (13.65–58.80 µm) remained below the 150 µm complete-arch misfit threshold.
Prott 2025 (56)	4	Micron-Mapper (SIN 360)	Primescan; Primescan + OptiSplint	Trueness RMS mean±SD: PG 20.5±0.6 µm, Primescan+OptiSplint 30.9±16.8 µm, and Primescan 56.0±0.7 µm; PG vs Primescan P<.001 and OptiSplint vs Primescan P=.004. Precision RMS: PG 6.0±1.2 µm, Primescan 9.5±3.3 µm, and Primescan+OptiSplint 23.3±22.3 µm; overall P=.192.

Table 2. Risk of bias assessment of included studies.

Study ID	RoB tool	Patient / model selection	Index test	Reference standard	Flow & timing	Overall risk of bias
Yan 2023	QUADAS-2	Some concerns	Low	Low	High	High
Fu 2025	QUADAS-2	Low	Low	Low	Low	Low
Santamaría-Laorden 2025	QUADAS-2	Some concerns	Low	Low	Low	Some concerns
Revilla-León 2025	QUADAS-2	Low	Low	Low	Low	Low
Revilla-León 2025 (clinical PG vs splinting)	QUADAS-2	High	Low	Low	Low	High
Pinto 2024	QUADAS-2	Low	Low	Low	Low	Low
Ke 2024	QUADAS-2	Some concerns	Some concerns	Low	Low	Some concerns

DOI: 10.18502/jcr.v13i3.23103

Study ID	RoB tool	Patient / model selection	Index test	Reference standard	Flow & timing	Overall risk of bias
Cheng 2024	QUADAS-2	Some concerns	Some concerns	Low	Low	Some concerns
Zhou 2024	QUADAS-2	Some concerns	Some concerns	Low	Low	Some concerns
Tohme 2021	QUADAS-2	Some concerns	Some concerns	Low	Low	Some concerns
Eldabe 2025	QUADAS-2	Some concerns	Some concerns	Low	Low	Some concerns
BrakoČ 2025	QUADAS-2	Some concerns	Low	Some concerns	Low	Some concerns
Fu 2024	QUADAS-2	Low	Some concerns	Low	Low	Some concerns
Jiranaphawiboon 2025	QUADAS-2	Some concerns	Some concerns	Low	Low	Some concerns
Zhang 2023	QUADAS-2	Some concerns	Some concerns	Low	Low	Some concerns
Lyu 2025	QUADAS-2	Some concerns	Some concerns	Low	Low	Some concerns
Liu 2024	QUADAS-2	Some concerns	Some concerns	Low	Low	Some concerns
Revilla-León 2025	QUADAS-2	Some concerns	Some concerns	Low	Low	Some concerns
Revilla-León 2025	QUADAS-2	Some concerns	Some concerns	Low	Low	Some concerns
Revilla-León 2025	QUADAS-2	High	Some concerns	Low	Low	High
Sallorenzo 2022	QUADAS-2	Some concerns	Some concerns	Low	Low	Some concerns
Tohme 2023	QUADAS-2	Some concerns	Some concerns	Low	Low	Some concerns
Revilla-León 2021	QUADAS-2	Some concerns	Some concerns	Low	Low	Some concerns
Abuduwaili 2025	QUADAS-2	Some concerns	Some concerns	Low	Low	Some concerns
Santamaría-Laorden 2025	QUADAS-2	Some concerns	Some concerns	Low	Low	Some concerns
Gómez-Polo 2025	QUADAS-2	Some concerns	Some concerns	Low	Low	Some concerns
Revilla-León 2025	QUADAS-2	Some concerns	Some concerns	Low	Low	Some concerns
Bin Farrah 2025	QUADAS-2	Some concerns	Some concerns	Low	Low	Some concerns
Muslu 2025	QUADAS-2	Some concerns	Some concerns	Low	Low	Some concerns
Bratos 2018	QUADAS-2	Some concerns	Some concerns	Low	Low	Some concerns
Chen 2024	QUADAS-2	Some concerns	Some concerns	Low	Low	Some concerns
Pozzi 2025	QUADAS-2	Some concerns	Some concerns	Low	Low	Some concerns
Revilla-León 2024	QUADAS-2	Some concerns	Some concerns	Low	Low	Some concerns
Bergin 2013	QUADAS-2	Some concerns	Some concerns	Low	Low	Some concerns
Orejas-Pérez 2022	QUADAS-2	High	Some concerns	High	Low	High
Benabdallah-M'Rabat 2025	QUADAS-2	Some concerns	Some concerns	Low	Low	Some concerns
Revilla-León 2025	QUADAS-2	Some concerns	Some concerns	Low	Low	Some concerns
Revilla-León 2025 – implant reference	QUADAS-2	Some concerns	Some concerns	Low	Low	Some concerns

Study ID	RoB tool	Patient / model selection	Index test	Reference standard	Flow & timing	Overall risk of bias
Pozzi 2025 – IPG trueness	QUADAS-2 (modified, in-vitro)	Some concerns	Some concerns	Low	Low	Some concerns
Wang 2023	QUADAS-2	High	Some concerns	Some concerns	Low	High
Negreiros 2025	QUADAS-2	Low	Some concerns	High	Low	High
Faria 2025	Modified QUADAS-2 (in vitro)	Low	Some concerns	High	Low	High
Estibalez-Recasens 2025	Modified QUADAS-2 (clinical)	Low	Some concerns	High	Low	High
Revilla-León 2025	Modified QUADAS-2 (in vitro)	Low	Some concerns	Low	Low	Some concerns
Revilla-León 2023	Modified QUADAS-2 (in vitro)	Low	Some concerns	Low	Low	Some concerns
Demirel 2023	Modified QUADAS-2 (in vitro)	Low	Some concerns	Low	Low	Some concerns
Faria 2025	Modified QUADAS-2 (in vitro)	Low	Some concerns	Low	Low	Some concerns
Prott 2025	Modified QUADAS-2 (in vitro)	Some concerns	Low	Low	Low	Some concerns

Table 3. Outcome-level GRADE Summary of Findings after 48-study reconciliation.

Outcome domain	Contributing studies*	Key evidence	Certainty	Interpretation
Clinical accuracy (trueness): PG/IPS/SPG vs IOS (distance/ ΔEUC/RMS + angular)	4	ΔEUC: IOS 59.8±30 μm vs IPS 30.7±18 μm; Angular: IOS 1.4±0.44° vs IPS 0.78±0.27°. Another study: RMS IOS 69 μm vs SPG 45 μm (p<.01); Angle IOS 0.40° vs SPG 0.31° (p<.01); Distance IOS 75 μm vs SPG 60 μm (p=.15).	⊕⊕◯◯ Low	Low certainty; favorable results in selected comparisons do not establish general clinical superiority.
Clinical precision: PG vs IOS (cross-over) (3D "Spatial Fit", cross-arch, terminal implant)	1	3D Spatial Fit mean±SD: IOS 61±54 μm vs PG 7±5 μm; Terminal implant (Virtual Sheffield) mean±SD: IOS 447±420 μm vs PG 38±31 μm (all p<0.0001).	⊕⊕⊕◯ Moderate	Moderate certainty, but all endpoints come from one 19-participant cross-over study.
Clinical repeatability/precision of PG measurements (linear + angular)	2	PIC stereophotogrammetry precision: linear 14.71±12.21 μm (0–61; none >75 μm) and angular 0.072±0.064° (0–0.345; none >0.6°). PIC app vs PIC system absolute difference: 21±16 μm and 0.20±0.17°.	⊕⊕◯◯ Low	Low certainty; small samples and limited devices restrict generalizability.
In vitro implant-position accuracy (trueness/precision): PG/IPG/EPG vs IOS/CNV	35	Mixed direction. Examples: PG better than IOS in some (e.g., PG-1 25.23 μm vs IOS 77.58 μm), but PG worse than IOS/CNV in others (e.g., PG 77.6 μm vs CNV 11.7 μm vs IOS 18.4–21.1 μm; Caramês trueness median RMS: Medit i500 24.45 μm, Trios 3 29.20 μm, PIC PG 49.45 μm, p<0.001). Prott et al. added a device-specific in-vitro comparison (trueness RMS: PG 20.5±0.6 μm vs Primescan 56.0±0.7 μm; precision comparison P=.192).	⊕◯◯◯ Very low	Very low certainty for clinical inference; mixed, heterogeneous, and indirect evidence.

DOI: 10.18502/jcr.v13i3.23103

Outcome domain	Contributing studies*	Key evidence	Certainty	Interpretation
Registration accuracy (soft-tissue ↔ implant-position scan registration)	2	Mean±SD discrepancies around ~103–127 µm: e.g., iCam4D 106±28 µm; OxoFit 103±38 µm; Grammee 116±52 µm; Elite 116±21 µm (ANOVA P=.270).	⊕⊕◯◯ Low	Low certainty; surrogate laboratory workflow outcome.
Time efficiency (capture/scanning time)	2	IPG 50.30±6.77 s and EPG 57.40±5.19 s vs IOS 91.10±20.31 s and IOSA 125.00±18.74 s ($p<0.001$).	⊕◯◯◯ Very low	Very low certainty; two device-specific laboratory studies.
Prosthesis/framework fit outcomes after PG-based workflows	2	Two included clinical studies contributed direct prosthesis/framework outcomes: 21/21 frameworks were reported to have acceptable passive fit in one prospective study, and one single-case workflow reported cumulative RMS deviation of 140.4 µm.	⊕◯◯◯ Very low	Very low certainty; two clinical reports, including one single case.

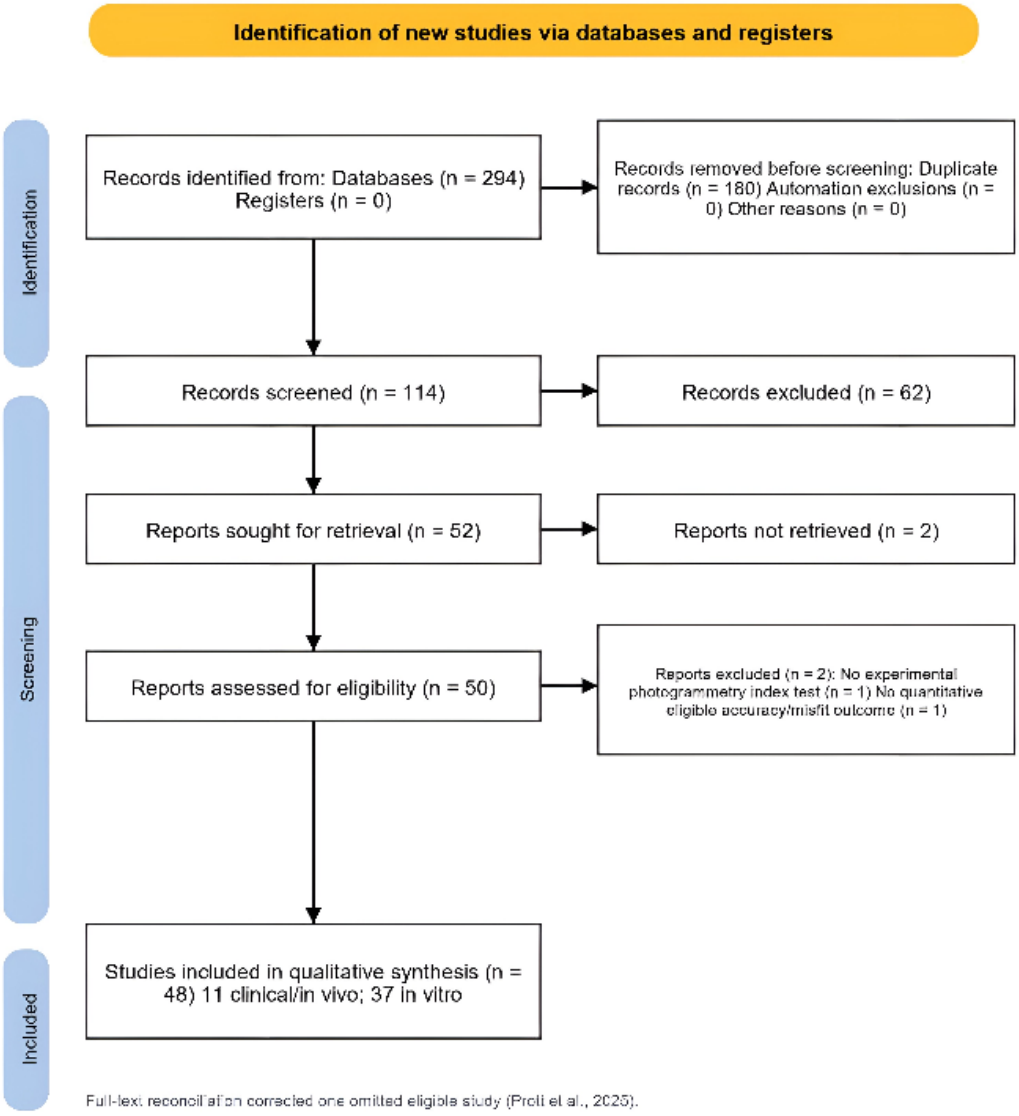


Figure 1. PRISMA flow diagram after full-text reconciliation (48 included studies).

Discussion

The evidence indicates that photogrammetry can achieve high repeatability and favorable trueness in selected complete-arch workflows; however, the strength of this conclusion changes materially after considering risk of bias, indirectness, and evidence independence. Only 3 of 48 studies were at low overall risk of bias, and all three were in vitro. Consistent with this profile, six of the seven formal GRADE outcome domains were low or very low certainty. Photogrammetry should therefore be viewed as a promising, protocol-sensitive capture method rather than an approach with established clinical superiority. The strongest comparative clinical precision signal came from Negreiros et al., a within-patient cross-over study of 19 completely edentulous arches. Photogrammetry showed lower variability than IOS across spatial-fit, cross-arch, and virtual Sheffield endpoints. These endpoints support one moderate-certainty domain, but they arise from the same participants and are not independent confirmations.

The study lacked an external trueness reference, used a single operator, and compared one photogrammetry system with one IOS platform; it therefore supports a possible precision advantage without establishing broader clinical superiority. A coherent explanation for these concordant clinical observations is that photogrammetry targets implant geometry directly and therefore limits cumulative distortion over edentulous spans—an issue that becomes more prominent as inter-implant distance increases and anatomic "texture" is reduced [21]. External/context evidence from a recent systematic review and meta-analysis likewise indicates that photogrammetry often outperforms IOS in complete-arch implant impressions, while emphasizing between-study heterogeneity and method dependence [1]. External/context evidence from another systematic review/meta-analysis similarly supports an overall advantage for photogrammetry in complete-arch digital implant impressions, but highlights that effect direction can vary with system type, scan strategy, and reference standard [4]. External/context evidence from implant-focused reviews of IOS accuracy (including in-vivo evidence) reinforces that accuracy is setting- and span-dependent, which aligns with the pattern that differences between workflows are most apparent in full-arch scenarios [49]. Discordant findings were most prominent in laboratory studies, where conventional impressions or specific IOS systems sometimes matched or exceeded photogrammetry depending on the alignment strategy, endpoint, and metrology reference.

Prott et al. (2025), added during reconciliation, reported better trueness for MicronMapper photogrammetry than Primescan, but the precision comparison was nonsignificant and used only five scans per group; its precision evidence was therefore rated very low certainty. Together, these findings reinforce that IOS and photogrammetry are families of device- and protocol-specific workflows, not fixed comparators [56]. A key contribution of the included evidence is that implant reference selection, capture distance, ambient lighting, camera position, implant angulation, and scan-body spacing can shift measured accuracy. These factors plausibly explain differences among studies and limit device-independent generalization. Implant reference selection, for example, produced measurable changes in reported discrepancies in a controlled assessment of a photogrammetry system, implying that "settings" can become an unrecognized source of bias when methods are underreported [37]. Similarly, a dedicated distance experiment showed that scanning distance influenced trueness for complete-arch implant scans, even where precision remained comparatively stable [10]. Environmental acquisition factors appear relevant as well: ambient lighting altered trueness for an intraoral photogrammetry-capable platform, supporting the need to standardize capture conditions when comparing systems [35].

Camera position and implant angulation were also shown to affect photogrammetry accuracy, which is consistent with evidence that implant angulation can modulate performance differences between photogrammetry and IOS [16,34]. From a clinical standpoint, a recurring challenge is that deviation metrics (RMS/linear/angular) are necessary but not sufficient surrogates for "passive fit," and only a minority of studies connected capture discrepancies to downstream outcomes such as adjustment burden, verification indices, or mechanical complications [31]. External/context evidence suggests that clinically acceptable misfit thresholds for complete-arch implant prostheses are not universal across materials, frameworks, and measurement approaches, which limits direct translation of a given µm-level discrepancy into a single actionable cutoff [50]. External/context evidence further indicates that framework misfit is associated with biomechanical sequelae and maintenance requirements, but also emphasizes substantial methodological variability in how misfit is defined and quantified across studies [51].

Limitations of the evidence

Most included studies were in vitro (37/48) and used

DOI: 10.18502/jcr.v13i3.23103

diverse reference standards, superimposition strategies, devices, and endpoints. Methodological reporting was uneven, consistent with 37 some-concerns and 8 high-risk ratings. The formal GRADE profile was correspondingly limited: only one of seven domains was moderate certainty, and that domain was based on a single clinical cross-over study. These limitations preclude a confident claim that photogrammetry is clinically superior across devices, protocols, or patient populations. Single-study evidence requires particular caution. The moderate-certainty clinical precision domain, time-efficiency comparisons, registration workflows, and prosthesis-level fit were each informed by one or a small number of studies, and several rows represented multiple outcomes from the same participants. These findings are hypothesis-generating until independently replicated.

Limitations of the review processes

The review was restricted to English-language publications and study authors were not contacted for missing or unclear information. Two full-text reports could not be retrieved for assessment, which may have introduced selection-related uncertainty if those reports differed systematically from included studies. Meta-analysis was not performed because of heterogeneity in systems, reference standards, and outcome metrics, and reporting-bias assessment therefore remained qualitative.

Implications for practice, policy, and future research

In practice, this review supports a cautious, conditional interpretation. Photogrammetry may be useful when long-span repeatability is a priority, but the evidence does not justify replacing established verification and fit-assessment procedures or assuming that one system's performance applies to another. Clinicians should interpret small scan deviations in the context of the specific device, capture protocol, reference method, and prosthetic verification workflow. For policy and standardization, the field would benefit from clearer consensus on (i) reference standards, (ii) reporting of acquisition conditions (distance, lighting, camera position), and (iii) a minimum outcome set that includes both trueness and precision with transparent alignment procedures. Future research should prioritize well-designed, adequately powered clinical head-to-head comparisons across representative photogrammetry systems and modern IOS platforms, using prespecified reference standards and reporting both immediate accuracy and downstream prosthesis-level outcomes (adjustment time, remakes, verification indices, maintenance events). Studies should also explicitly test protocol variables (implant reference selection, scan distance, lighting, and implant angulation) under controlled conditions and report them as reproducible parameters, because current evidence indicates these factors can meaningfully shift measured trueness.

Conclusion

Photogrammetry shows a plausible precision advantage for complete-arch implant capture in selected workflows, but current confidence is limited. The evidence is dominated by in-vitro studies, only 3 of 48 studies were at low risk of bias, and six of seven GRADE outcome domains were low or very low certainty. The sole moderate-certainty domain arose from one 19-participant cross-over study and awaits independent replication. Photogrammetry should therefore be considered a promising adjunct rather than a universally superior replacement for IOS or conventional impressions, with continued prosthetic verification and protocol-specific validation required.

Conflict of Interest

There is no conflict of interest to declare.

References

[1] Altalla H, Alhelou H, Karaduman F, Alawawda O, Bayindir F. Comparative accuracy of photogrammetry and intraoral scanners in recordings for complete arch implant-supported prostheses: A systematic review and meta-analysis. J Prosthet Dent. 2025.

[2] Cheng J, Zhang H, Liu H, Li J, Wang H, Tao X. Accuracy of edentulous full-arch implant impression: An in vitro comparison between conventional impression, intraoral scan with and without splinting, and photogrammetry. Clin Oral Implant Res. 2024; 35(5):560–72.

[3] Negreiros WM, Akhondi S, Quiles HK, Hamilton A. Photogrammetry in Implant Dentistry. Aust Dent J. 2025; 70(S1):S15–S24.

[4] Pozzi A, Arcuri L, Carosi P, Laureti A, Londono J, Wang H-L. Photogrammetry Versus Intraoral Scanning in Complete-Arch Digital Implant Impression: A Systematic Review and Meta-Analysis. Clin Implant Dent Relat Res. 2025; 27(3):e70059.

[5] Abuduwaili K, Huang R, Song J, Liu Y, Chen Z, Huang B, et al. Comparison of photogrammetric

imaging, intraoral scanning and conventional impression accuracy of full-arch dental implant rehabilitation: an in vitro study. BMC Oral Health. 2025; 25(1):753.

[6] Peñarrocha-Oltra D, Agustín-Panadero R, Bagán L, Giménez B, Peñarrocha M. Impression of multiple implants using photogrammetry: description of technique and case presentation. Med Oral Patol Oral Cir Bucal. 2014; 19(4):e366–71.

[7] Revilla-León M, Gómez-Polo M, Drone M, Barmak A, Att W, Kois J, et al. Influence of implant reference on the scanning accuracy of complete arch implant scans captured by using a photogrammetry system. J Prosthet Dent. 2025; 133(1):252–7.

[8] Revilla-León M, Barmak AB, Drone M, Kois JC, Alonso Pérez-Barquero J. Capturing complete arch implant positions in two partial photogrammetry scans: Does it impact the accuracy of complete arch implant scans? J Prosthet Dent. 2025.

[9] Revilla-León M, Cascos-Sanchez R, Barmak AB, Drone M, Kois JC, Gómez-Polo M. Accuracy of complete arch implant scans recorded by using intraoral and extraoral photogrammetry systems and a noncalibrated splinting technique: A clinical study. J Prosthet Dent. 2025.

[10] Revilla-León M, Gómez-Polo M, Drone M, Barmak A, Guinot-Barona C, Att W, et al. Impact of scanning distance on the accuracy of a photogrammetry system. J Dent. 2024; 142:5.

[11] Fu X, Cai Z, Shi J, Qiao S, Tonetti M, Lai H, et al. Accuracy of a Novel Intraoral Photogrammetry Technique for Complete-Arch Implant Impressions: An In Vitro Study. Clin Oral Implant Res. 2025; 36(8):991–9.

[12] Estibalez-Recasens M, Serrano-Granger C, Santamaría-Laorden A, Andreu-Vázquez C, Orejas-Pérez J. Precision of stereophotogrammetry in complete arch implant recordings: A clinical study. The Journal of Prosthetic Dentistry. 2025; 133(5):1242–9.

[13] Faria JC, Sampaio-Fernandes MA, Oliveira SJ, Malheiro R, Sampaio-Fernandes JC, Figueiral MH. Precision of Photogrammetry and Intraoral Scanning in Full-Arch Implant Rehabilitation: An In Vitro Comparative Study. Applied Sciences. 2025; 15(3):1388.

[14] Jiranaphawiboon A, Rokaya D, Sanohkan S. Accuracy of one-versus two-phase photogrammetry implant impression system: an in-vitro study. The Saudi Dental Journal. 2025; 37(7):42.

[15] Lohatchwanit S, Narkbuakaew W, Aunmeungtong W, Khongkhunthian P. The accuracy of stereophotogrammetric, intraoral scanning, and conventional open-tray impression techniques for complete arch fixed implant-supported prostheses: An in vitro study. Digital Dentistry Journal. 2025; 2(2):100035.

[16] Muslu T, Kurtulmus-Yilmaz S. Effect of implant angulation on the trueness and precision of intraoral scanning and photogrammetry. BMC Oral Health. 2025; 25(1):1739.

[17] Yan Y, Lin X, Yue X, Geng W. Accuracy of 2 direct digital scanning techniques-intraoral scanning and stereophotogrammetry-for complete arch implant-supported fixed prostheses: A prospective study. J Prosthet Dent. 2023; 130(4):564–72.

[18] Santamaría-Laorden A, Castillo-De-Oyagüe R, Martínez-Marugán A, Andreu-Vázquez C, Orejas-Pérez J. Accuracy of a smartphone app and photogrammetry algorithm in complete arch digital implant capture: An in vivo comparative study. J Prosthet Dent. 2025.

[19] Revilla-León M, Cascos R, Barmak AB, Drone M, Kois JC, Gómez-Polo M. Clinical accuracy of complete arch implant scans recorded by using a noncalibrated splinting technique, intraoral photogrammetry, and extraoral photogrammetry with snap-on markers. J Prosthet Dent. 2025.

[20] Eldabe AK, Adel-Khattab D, Botros KH. Accuracy of intraoral photogrammetry in complete arch digital implant scanning: An in vivo prospective comparative study. J Prosthet Dent. 2025.

[21] Fu XJ, Liu M, Liu BL, Tonetti MS, Shi JY, Lai HC. Accuracy of intraoral scan with prefabricated aids and stereophotogrammetry compared with open tray impressions for complete-arch implant-supported prosthesis: A clinical study. Clin Oral Implant Res. 2024; 35(8):830–40.

[22] Zhang YJ, Qian SJ, Lai HC, Shi JY. Accuracy of photogrammetric imaging versus conventional impressions for complete arch implant-supported fixed dental prostheses: A comparative clinical study. J Prosthet Dent. 2023; 130(2):212–8.

[23] Orejas-Pérez J, Giménez González B, Ortiz-Colla-

 DOI: 10.18502/jcr.v13i3.23103

do I, Thuissard-Vasallo IJ, Santamaría-Laorden A. In Vivo Complete-Arch Implant Digital Impressions: Comparison of the Precision of Three Optical Impression Systems. Int J Environ Res Public Health. 2022; 19(7).

[24] Wang J, Wu Y, Ma J, Wu F, Li D. A novel technique for implant-supported fixed complete rehabilitation based on a dynamic virtual patient. J Dent. 2023; 137:5.

[25] Negreiros W, Sun T, Jain S, Finkelman M, Gallucci G, Hamilton A. Precision of complete-arch digital implant scans using photogrammetry and intra-oral scanning. An in vivo cross-over study Complete-Arch Implant Scans: Photogrammetry vs IOS. J Dent. 2025; 161:10.

[26] Pinto R, Casado S, Chmielewski K, Carames J, Marques D. Accuracy of different digital acquisition methods in complete arch implant-supported prostheses: An in vitro study. J Prosthet Dent. 2024; 132(1):172–7.

[27] Tohme H, Lawand G, Eid R, Ahmed K, Salameh Z, Makzoume J. Accuracy of Implant Level Intraoral Scanning and Photogrammetry Impression Techniques in a Complete Arch with Angled and Parallel Implants: An In Vitro Study. Appl Sci-Basel. 2021; 11(21):11.

[28] Revilla-León M, Att W, Özcan M, Rubenstein J. Comparison of conventional, photogrammetry, and intraoral scanning accuracy of complete-arch implant impression procedures evaluated with a coordinate measuring machine. J Prosthet Dent. 2021; 125(3):470–8.

[29] Pozzi A, Laureti A, Tawil I, Chow J, Azevedo L, Fehmer V, et al. Intra Oral Photogrammetry: Trueness Evaluation of Novel Technology for Implant Complete-Arch Digital Impression In Vitro. Clin Implant Dent Relat Res. 2025; 27(3).

[30] Revilla-León M, Rubenstein J, Methani M, Piedra-Cascón W, Özcan M, Att W. Trueness and precision of complete-arch photogrammetry implant scanning assessed with a coordinate-measuring machine. J Prosthet Dent. 2023; 129(1):160–5.

[31] Demirel M, Donmez M, Sahmali S. Trueness and precision of mandibular complete-arch implant scans when different data acquisition methods are used. J Dent. 2023; 138:7.

[32] Lyu M, Li Y, Xu D, Xing Q, Zhang S, Yuan Q. Accuracy of Photogrammetry, Intraoral Scanning, and Conventional Impression for Multiple Implants: An In Vitro Study. Clin Implant Dent Relat Res. 2025; 27(1).

[33] Tohme H, Lawand G, Chmielewska M, Makhzoume J. Comparison between stereophotogrammetric, digital, and conventional impression techniques in implant-supported fixed complete arch prostheses: An in vitro study. J Prosthet Dent. 2023; 129(2):354–62.

[34] Benabdallah-M'Rabat M, Santamaria-Laorden A, Bertuol-Gessi S, Martínez-Marugán A, Suarez-Garcia A, Thuissard I, et al. Influence of camera position, implant angulation and implant reference on the accuracy of complete arch implant recordings with photogrammetry. J Adv Prosthodont. 2025; 17(5):292–303.

[35] Gómez-Polo M, Revilla-León M, Herranz-Seijo P, Antonaya-Martín JL, Barmak AB, Cascos R. Do ambient lighting conditions affect the accuracy of implant position capture for complete arch prostheses using intraoral photogrammetry? J Prosthet Dent. 2025.

[36] Bin Farrah A, Ahmadian L, Shonberg D, Harlow R, Yang B. Effect of angulation between multi-unit abutments on trueness of photogrammetry systems. J Prosthodont. 2025:8.

[37] Revilla-León M, Gómez-Polo M, Drone M, Barmak AB, Kois JC, Alonso Pérez-Barquero J. Accuracy of complete arch implant scans recorded by using intraoral and extraoral photogrammetry systems. J Prosthet Dent. 2025.

[38] Ke Y, Zhang Y, Tian S, Chen H, Sun Y. Accuracy of digital implant impressions using a novel structured light scanning system assisted by a planar mirror in the edentulous maxilla: An in vitro study. Clin Oral Implant Res. 2024; 35(8):876–87.

[39] Zhou Y, You L, Fan Z. Accuracy of implant abutment level digital impressions using stereophotogrammetry in edentulous jaws: an in vitro pilot study. BMC Oral Health. 2024; 24(1).

[40] Brakoc J, Todorovic A, Mangano F, Glisic M, Scepanovic M. Accuracy of intraoral photogrammetry versus direct digital implant impressions in the fully edentulous lower jaw: An in vitro study. J Dent. 2025; 156:8.

[41] Liu M, Fu XJ, Lai HC, Shi JY, Liu BL. Accuracy

of traditional open-tray impression, stereophotogrammetry, and intraoral scanning with prefabricated aids for implant-supported complete arch prostheses with different implant distributions: An in vitro study. J Prosthet Dent. 2024; 132(3):602–.e9.

[42] Revilla-León M, Cascos R, Barmak A, Kois J, Gómez-Polo M. Alignment accuracy of soft tissue and implant position scans captured by using four intraoral scanners and an intraoral photogrammetry system with and without coded healing abutments. J Prosthet Dent. 2025; 134(4):10.

[43] Sallorenzo A, Gomez-Polo M. Comparative study of the accuracy of an implant intraoral scanner and that of a conventional intraoral scanner for-arch fixed dental. J Prosthet Dent. 2022; 128(5):1009–16.

[44] Santamaría-Laorden A, Marugán A, Andreu-Vázquez C, Orejas-Pérez J. Complete arch implant capture using a photogrammetry algorithm and smartphone app: An in vitro study. J Dent. 2025; 161:8.

[45] Revilla-León M, Barmak AB, Rokhshad R, Lawand G, Kois JC, Alonso Pérez-Barquero J. Does the interimplant scan body distance impact the scanning accuracy of an intraoral photogrammetry system? J Prosthet Dent. 2025.

[46] Bratos M, Bergin J, Rubenstein J, Sorensen J. Effect of simulated intraoral variables on the accuracy of a photogrammetric imaging technique for complete-arch implant prostheses. J Prosthet Dent. 2018; 120(2):232–41.

[47] Chen Y, Zhu M, He B, Deng Z. Efficient intraoral photogrammetry using self-identifying projective invariant marker. Int J Comput Assist Radiol Surg. 2024; 19(4):767–78.

[48] Pozzi A, Arcuri L, Laureti A, Carosi P, Gallucci G, Londono J. Image-guided photogrammetry accuracy: In vitro evaluation of an implant-supported complete arch digital scanning technology. J Prosthet Dent. 2025; 134(3):818–28.

[49] Bergin JM, Rubenstein J, Mancl L, Brudvik JS, Raigrodski AJ. An in vitro comparison of photogrammetric and conventional complete-arch implant impression techniques. J Prosthet Dent. 2013; 110(4):243–51.

[50] Revilla-León M, Barmak A, Lanis A, Kois J. Influence of connected and nonconnected calibrated frameworks on the accuracy of complete arch implant scans obtained by using four intraoral scanners, a desktop scanner, and a photogrammetry system. J Prosthet Dent. 2025; 134(3):800–8.

[51] Revilla-León M, Cascos R, Barmak AB, Kois JC, Gómez-Polo M. Registration accuracy of soft tissue information scan captured using an intraoral scanner and implant position scan recorded using extraoral and intraoral photogrammetry systems. J Prosthet Dent. 2025.

[52] Faria JC, Sampaio-Fernandes MA, Oliveira SJ, Malheiro R, Sampaio-Fernandes JC, Figueiral MH. Trueness of Implant Positioning Using Intraoral Scanning and Dental Photogrammetry for Full-Arch Implant-Supported Rehabilitations: An In Vitro Study. Appl Sci. 2025; 15(14).

[53] Ma J, Zhang B, Song H, Wu D, Song T. Accuracy of digital implant impressions obtained using intraoral scanners: a systematic review and meta-analysis of in vivo studies. International Journal of Implant Dentistry. 2023; 9(1):48.

[54] Pesce P, Nicolini P, Caponio VCA, Zecca PA, Canullo L, Isola G, et al. Accuracy of Full-Arch Intraoral Scans Versus Conventional Impression: A Systematic Review with a Meta-Analysis and a Proposal to Standardise the Analysis of the Accuracy. Journal of Clinical Medicine. 2025; 14(1):71.

[55] Abdelrehim A, Etajuri EA, Sulaiman E, Sofian H, Salleh NM. Magnitude of misfit threshold in implant-supported restorations: A systematic review. The Journal of Prosthetic Dentistry. 2024; 132(3):528–35.

[56] Prott LS, Atria PJ, Maluf CV, Blatz MB, Conejo J. In vitro comparison between complete arch abutment-level implant impressions with photogrammetry, grammetry, and intraoral scanning. J Prosthet Dent. 2025; 134:782.e1-782.e7. doi:10.1016/j.prosdent.2025.05.009.

 DOI: 10.18502/jcr.v13i3.23103